Nonperturbative aspects of the quark-photon vertex

M. R. Frank
Institute for Nuclear Theory, University of Washington, HN-12, Seattle, Washington 98195
(Received 2 March 1994)

The electromagnetic interaction with quarks is investigated through a relativistic, electromagnetic gauge-invariant treatment. Gluon dressing of the quark-photon vertex and the quark self-energy functions is described by the inhomogeneous Bethe-Salpeter equation in the ladder approximation and the Schwinger-Dyson equation in the rainbow approximation, respectively. Results for the calculation of the quark-photon vertex are presented in both the timelike and spacelike regions of photon momentum squared; however, emphasis is placed on the spacelike region relevant to electron scattering. The treatment presented here simultaneously addresses the role of dynamically generated $q\bar{q}$ vector bound states and the approach to asymptotic behavior. The resulting description is therefore applicable over the entire range of momentum transfers available in electron scattering experiments. Input parameters are limited to the model gluon two-point function, which is chosen to reflect confinement and asymptotic freedom, and are largely constrained by the obtained bound-state spectrum.

PACS number(s): 24.85.+p, 13.60.Le

I. INTRODUCTION

As hadrons are subjected to more detailed examination in electron scattering experiments, such as those proposed at CEBAF, a quark-based description of their electromagnetic (EM) interaction, which is applicable over a broad range of momenta, becomes desirable. Local effective field theories based on hadronic degrees of freedom, although attractive for their efficiency, are subject to difficulties when conditions are sufficient to probe characteristics of subhadronic origin [1]. An ideal perspective on this problem can be gained by sacrificing local interactions in favor of retaining some knowledge of the quark substructure content of the effective hadron fields [2], and is the spirit of the present investigation. In such a treatment, the EM interaction with a pion at tree level in the hadron fields is, for example, illustrated in Fig. 1. There, the pion Bethe-Salpeter amplitudes Γ reflect the ability of the internal degrees of freedom to share the transferred momentum, while the quark-photon vertex (QPV) Γ_ν contains information about the interaction with a dressed quark, including the production of $q\bar{q}$ vector-meson modes expected from vector-meson dominance or dispersion theory phenomenology. At larger momentum transfers where the effective scale provided by the vector-meson poles has been exceeded, the QPV also provides information about the approach of photon-hadron vertices to asymptotic behavior. A quantitative understanding of the QPV is therefore central to the EM description of hadrons at intermediate momentum scales, and must address issues of confinement, dynamically generated $q\bar{q}$ vector bound states, and asymptotic freedom.

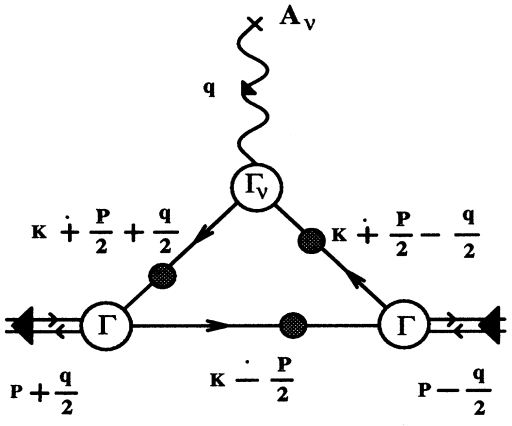

FIG. 1. The EM vertex for a composite pion at tree level. The quark Green's functions QPV and the pion Bethe-Salpeter amplitudes are dressed in a consistent, gauge-invariance manner.

In addition to its role in the EM interaction, the QPV is a quantity of interest on its own merit. It is well known, for example, that a formal description of meson bound-state spectra and wave functions can be obtained by considering the interaction of a quark with an external field having the quantum numbers of the bound state of interest. In such a description, the external field excites a $q\bar{q}$ pair from the vacuum. Their subsequent gluon-mediated interactions provide self-energy and vertex dressing. The existence of bound states is exhibited by poles in the dressed vertex. The position and residue of a given pole yield information about the bound-state mass and wave function respectively. Vertex functions of quarks with external fields thus provide a unique environment in which to study the formation of meson bound states. The interaction with a photon is simply one example of this, and it is expected that the approach presented here can be applied to the description of bound states with other quantum numbers as well as vectors.

In this paper the QPV with gluon dressing at the ladder level of approximation is investigated in both the timelike and spacelike regions of photon momentum squared. Particular attention is given to the formation of vector bound states and confinement phenomenology,

however, the primary goal of this initial investigation is to develop a description of the quark-photon interaction in the spacelike region relevant to electron scattering which simultaneously addresses the role of vector mesons and quark substructure. The equations implied by the ladder approximation are[1] the inhomogeneous Bethe-Salpeter equation

$$\Gamma_\mu(P,q) = -i\gamma_\mu - \frac{4}{3}g^2\int\frac{d^4K}{(2\pi)^4}D(P-K)\gamma_\nu G(K_+) \times\Gamma_\mu(K,q)G(K_-)\gamma_\nu, \quad (1)$$

and the Schwinger-Dyson equation

$$\Sigma(P) = \frac{4}{3}g^2\int\frac{d^4K}{(2\pi)^4}D(P-K)\gamma_\nu G(K)\gamma_\nu, \quad (2)$$

where $K_\pm = K \pm q/2$, the quark Green's function, G, is defined from its inverse $G^{-1}(P) = i\not{P} + \Sigma(P)$, and for convenience the model gluon two-point function is taken to be diagonal in Lorentz indices ($D_{\mu\nu} = \delta_{\mu\nu}D$). In Eq. (1) q is the photon momentum, while P is the average of the incoming and outgoing quark momenta. These expressions are illustrated in Fig. 2. The current-quark masses in this investigation are assumed to be zero, which allows an overall charge matrix to be omitted from Eq. (1), but the approach can be easily extended to include nonzero masses. The absence of masses further implies that all dimensionful constants enter through the parametrization of the gluon two-point function, D. Here the infrared contribution to this quantity is characterized by an effective strength η and an effective range R_0, in addition to the known ultraviolet form.

The motivation for employing the ladder approximation is provided by the following arguments. First, it offers an EM gauge-invariant description. Both the Ward-Takahashi identity (WTI),

$$q_\mu\Gamma_\mu(P,q) = G^{-1}(P_-) - G^{-1}(P_+), \quad (3)$$

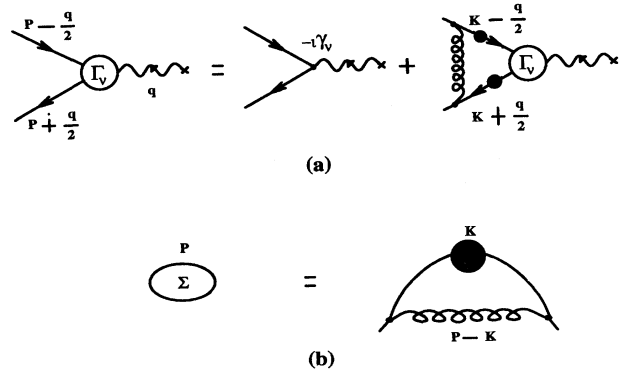

FIG. 2. The ladder approximation for (a) the QPV and (b) the quark self-energy. The Green's functions are defined by their inverse $G^{-1}(P) = i\not{P} + \Sigma(P)$.

[1]The Euclidean metric, in which $a\cdot a = a_\mu a_\mu$ and $\{\gamma_\mu,\gamma_\nu\} = 2\delta_{\mu\nu}$, is used throughout this work.

and the Ward identity (WI),

$$\Gamma_\mu(P,0) = -\frac{\partial G^{-1}(P)}{\partial P_\mu}, \quad (4)$$

are satisfied by this approximation. This is easily demonstrated by directly substituting (3) or (4) into (1) for the vertex, and employing (2). Further, it has been shown recently how gauge invariance at the quark level in the ladder approximation to the QPV fits into a gauge-invariant description of composite mesons leading to WTIs at the hadronic level [2].

Second, in the vicinity of a $q\bar{q}$ resonance, the vertex obtains the form

$$\Gamma_\mu(P,q) \approx \frac{M_V^2}{q^2+M_V^2}\Omega_\mu(P,q), \quad (5)$$

where Ω_μ is the residue at the pole, and, from (1), satisfies

$$\Omega_\mu(P,q) = -\frac{4}{3}g^2\int\frac{d^4K}{(2\pi)^4}D(P-K)\gamma_\nu G(K_+) \times\Omega_\mu(K,q)G(K_-)\gamma_\nu \quad (6)$$

for $q^2 = -M_V^2$. This is the homogeneous Bethe-Salpeter equation in the ladder approximation for a vector $q\bar{q}$ bound state. One can conclude from (3) and (5) that the on-mass-shell solution of the homogeneous equation satisfies $q_\mu\Omega_\mu(P,q) = 0$, provided the self-energy functions are nonsingular. The Bethe-Salpeter equation at this level has been investigated previously, and acceptable results have been obtained for the lowest mass bound states [3–6]. It is therefore anticipated that, in the addition to providing an EM gauge invariant description of the quark-photon interaction for use in electron scattering, this level of approximation has the ability to describe the spectrum and structure of vector bound states.

Finally, the Schwinger-Dyson equation (2) has been extensively studied with regard to confinement phenomenology and dynamical chiral symmetry breaking [7]. It has been demonstrated, for example, that for a suitably chosen gluon two-point function D, quark Green's functions which are free of singularities on the real P^2 axis are produced in the vacuum; therefore denying the existence of a single-particle spectrum. It is shown here, however, that this is not a sufficient condition for the formation of finite-size $q\bar{q}$ states, but is an essential ingredient in a description of confinement based on an interaction between dressed quarks which does not rise to infinity at large distances. This alternate description of confinement in fact relies on the interaction between dressed quarks diminishing at separations beyond the characteristic length scale R_0, at which point the quark Green's function approaches its vacuum value. The quarks are then repelled by the vacuum due to the absence of a mass pole in the vacuum quark Green's function. The effective "rising potential" of traditional models of confinement occurs here as a result of the repulsive interaction of quarks with the vacuum in combination with the decreasing interaction between dressed quarks with increasing separation. Such a description has proven successful in the formulation of

a confining nontopological soliton model for baryons [8]. There propagating quark modes are made possible by the baryon mean field. However, as a quark moves toward the edge of the baryon where the mean field vanishes, the constituent-quark mass rises to infinity. Quarks are thus confined to the region of nonzero mean field by virtue of their repulsive interaction with the vacuum. This mechanism arises naturally here, and is pursued as a possible realization of confinement.

The paper is organized as follows. In Sec. II the general features of the QPV are given along with the reduction of Eq. (1) to a form suitable for computer applications. The solution of the homogeneous Bethe-Salpeter equation (6) is also discussed there. In Sec. III a discussion of confinement is presented in the context of a particular model which yields analytic solutions to both the inhomogeneous Bethe-Salpeter and Schwinger-Dyson equations (1) and (2) respectively. Also discussed there is the criteria for the formation of finite-range bound states in the context of this model of confinement. The numerical evaluation of the QPV for both the timelike and spacelike regions of the photon momentum squared is given in Sec. IV. Finally, a summary is presented in Sec. V.

II. GENERAL FEATURES

A. The inhomogeneous Bethe-Salpeter equation

In this section, the steps required to reduce the inhomogeneous Bethe-Salpeter equation (1) to a form suitable for computer applications are outlined. The approach is straightforward and is based on the general features of the QPV as described by (1). Where possible, lengthy algebraic manipulations are omitted. To begin, it is useful to write the self-energy Σ from (2), in the form

$$\Sigma(P) = i\not{P}\left[A(P^2)-1\right] + B(P^2)\ , \tag{7}$$

where

$$\left[A(P^2)-1\right]P^2 = g^2\frac{8}{3}\int\frac{d^4K}{(2\pi)^4}D(P-K) \times \frac{A(K^2)P\cdot K}{K^2A^2(K^2)+B^2(K^2)} \tag{8}$$

and

$$B(P^2) = g^2\frac{16}{3}\int\frac{d^4K}{(2\pi)^4}D(P-K)\frac{B(K^2)}{K^2A^2(K^2)+B^2(K^2)}. \tag{9}$$

The quark Green's function G and its inverse G^{-1} can then be written as

$$G(P) = -i\not{P}\alpha(P^2)+\beta(P^2),$$
$$G^{-1}(P) = i\not{P}A(P^2)+B(P^2), \tag{10}$$

where α and β are defined in an obvious fashion from G^{-1}.

From Eq. (1) it is evident that the QPV, in addition to its Lorentz four-vector structure, is a four-by-four matrix in Dirac indices and is in general a function of two nonorthogonal four vectors, P and q ($P\cdot q \neq 0$). On first appraisal, one might therefore expect that the complete set of 16 Dirac matrices $\{\mathbf{1},\gamma_5,\gamma_\mu,\gamma_5\gamma_\mu,\sigma_{\mu\nu}\}$ must be employed in its description. However, by limiting the gluon two-point function D to diagonal components in Lorentz indices, the tensor $\sigma_{\mu\nu}$ is excluded. This is seen explicitly by rewriting the integrand of (1) using

$$[\gamma_\nu G(K_+)\Gamma_\mu(P,q)G(K_-)\gamma_\nu]_{il} = (\gamma_\nu)_{ij}\left[G(K_+)\Gamma_\mu(P,q)G(K_-)\right]_{jk}(\gamma_\nu)_{kl} = \frac{1}{4}M^a_{il}\mathrm{tr}\left[M^aG(K_+)\Gamma_\mu(P,q)G(K_-)\right], \tag{11}$$

where the set of matrices

$$M^a \equiv \left\{\mathbf{1}, i\gamma_5, i\gamma_\mu/\sqrt{2}, i\gamma_5\gamma_\mu/\sqrt{2}\right\}\ ,$$

from which $\sigma_{\mu\nu}$ is absent, is obtained through Fierz reordering, and the repeated indices are summed. Further, the pseudoscalar matrix γ_5 can be excluded by considering that the corresponding term in (11) has the form $\gamma_5\Lambda^5_\mu(P,q)$, where the matrix structure has been completely factored. In order to contribute to the QPV, this term must form a four vector, which requires $\Lambda^5_\mu(P,q)$ to be an axial vector. It is immediately evident that this is impossible since there is an insufficient number of four vectors (P and q) to combine with the tensor $\epsilon_{\mu\nu\alpha\beta}$ to form an axial vector. The solution to (1) must therefore have the general form

$$\Gamma_\mu(P,q) = \mathbf{1}\Lambda^{(1)}_\mu(P,q) + i\gamma_\nu\Lambda^{(2)}_{\nu\mu}(P,q) + i\gamma_5\gamma_\nu\epsilon_{\mu\nu\alpha\beta}P_\alpha q_\beta\eta^{-2}\Lambda^{(3)}(P,q), \tag{12}$$

where the matrix structure is now explicit and the quantities $\Lambda^{(i)}$ are dimensionless functions with Lorentz structure indicated by their indices. The constant η has dimension of $(\text{length})^{-1}$ and is associated with the infrared strength of the gluon two-point function.

The further reduction of the $\Lambda^{(i)}$ to a set of invariant functions is achieved through the use of the symmetry transformations of the vertex $\Gamma_\mu(P,q)$ under γ_5; charge conjugation, $\mathcal{C}=\gamma_2\gamma_4$; and parity, $\mathcal{P}=\gamma_4$. The transformation properties are determined directly from the inhomogeneous Bethe-Salpeter equation (1) and are given by

$$\begin{aligned}\gamma_5\Gamma_\mu(P,q)\gamma_5 &= -\Gamma_\mu(-P,-q)\ ,\\ \mathcal{C}\Gamma_\mu(P,q)\mathcal{C}^{-1} &= -\Gamma_\mu(-P,q)^t\ ,\\ \mathcal{P}\Gamma_\mu(P,q)\mathcal{P}^{-1} &= \omega_{\mu\nu}\Gamma_\nu(P_4;-\mathbf{P},q_4;-\mathbf{q})\ ,\end{aligned} \tag{13}$$

where $\omega_{\mu\nu}=\mathrm{diag}(-1,-1,-1,1)$ and t denotes a matrix transpose. From the general form given in (12) and the

first two expressions in (13), it is clear that $\Lambda^{(2)}_{\mu\nu}(P,q)$ and $\Lambda^{(3)}(P,q)$ are even in both P and q, while $\Lambda^{(1)}_{\mu}(P,q)$ is odd in P and even in q. The quantities $\Lambda^{(i)}$ can therefore be written as

$$\begin{aligned}
\Lambda^{(1)}_{\mu}(P,q) &= \frac{q_\mu}{\eta}\frac{P\cdot q}{q^2}\lambda_1^L + \frac{P^T_\mu}{\eta}\lambda_1^T, \\
\Lambda^{(2)}_{\nu\mu}(P,q) &= \frac{P_\nu q_\mu}{\eta^2}\frac{P\cdot q}{q^2}\lambda_2^L + \frac{P_\nu P^T_\mu}{\eta^2}\lambda_2^T \\
&\quad -\frac{q_\nu q_\mu}{q^2}\lambda_3^L - \left(\delta_{\nu\mu} - \frac{q_\nu q_\mu}{q^2}\right)\lambda_3^T \\
&\quad +\frac{q_\nu P^T_\mu P\cdot q}{\eta^4}\lambda_4^T, \\
\Lambda^{(3)}(P,q) &= \lambda_5^T .
\end{aligned} \tag{14}$$

Here the coefficients λ are functions of P^2, q^2, and C^2_{Pq} where $C_{Pq} \equiv P\cdot q/(Pq)$ is the direction cosine between P and q, and $P^T_\mu \equiv P_\mu - P\cdot q q_\mu/q^2$ is the vector transverse to q_μ ($P^T\cdot q = 0$). The behavior of the coefficients for large spacelike q^2 consistent with asymptotic freedom [9] can be anticipated from (12) and (14). In particular, as $q^2 \to \infty$ the coefficients $\lambda_3^{T,L}$ must tend to unity, while all others tend to zero. The separation in (14) into longitudinal and transverse contributions with respect to the index μ allows three of the eight coefficient functions, λ, to be immediately determined from the WTI (3) in terms of the self-energy functions A and B given in (8) and (9) respectively. The longitudinal coefficient functions are thus given by

$$\begin{aligned}
\frac{P\cdot q}{\eta}\lambda_1^L &= B(P^2_-) - B(P^2_+) , \\
\frac{P\cdot q}{\eta^2}\lambda_2^L &= A(P^2_-) - A(P^2_+) , \\
\lambda_3^L &= \frac{1}{2}\left[A(P^2_-) + A(P^2_+)\right] .
\end{aligned} \tag{15}$$

The additional constraint provided by the WI (4) obtains the soft-photon limits:

$$\begin{aligned}
\lambda_1^L\big|_{q=0} &= \lambda_1^T\big|_{q=0} = -2\eta B'(P^2) , \\
\lambda_2^L\big|_{q=0} &= \lambda_2^T\big|_{q=0} = -2\eta^2 A'(P^2) , \\
\lambda_3^L\big|_{q=0} &= \lambda_3^T\big|_{q=0} = A(P^2),
\end{aligned} \tag{16}$$

where the prime denotes differentiation with respect to the argument.

The five unknown transverse coefficients can be isolated using (12) and (14), and the orthogonality of the Dirac matrices. The closed set of equations so obtained can be written in matrix form as

$$b_i = \mathcal{N}_{ij}(P^2, C^2_{Pq}; q^2)\lambda_j^T(P^2, C^2_{Pq}; q^2) + \int_0^\infty dK K^3 \int_{-1}^{1} dC_{Kq}\mathcal{M}_{ij}(P^2, C^2_{Pq}, K^2, C^2_{Kq}; q^2)\lambda_j^T(K^2, C^2_{Kq}; q^2), \tag{17}$$

where $\mathcal{M}$ and $\mathcal{N}$ (b and λ^T) are matrices (vectors) in the five-component space of the coefficient functions and C_{Kq} is the direction cosine between K and q. The steps required to reach the result (17) along with the explicit forms of $\mathcal{M}$, $\mathcal{N}$, and b are given in the Appendix. Equation (17) contains the same information as the transverse component of the inhomogeneous Bethe-Salpeter equation (1); to this point, no approximations have been made. To proceed further requires the specification of the gluon two-point function, D.

B. The homogeneous Bethe-Salpeter equation

The solutions of the homogeneous Bethe-Salpeter equation (6) describe the coupling of a $q\bar{q}$ vector bound state to a quark, and thereby provide information about the internal dynamics of the bound state. Although these solutions can be obtained directly from the coefficient functions λ_i^T of the preceding section, their normalization is more readily achieved by considering the solution of the homogeneous equation. To this end, the quantity $\Omega_\mu(P,q)$ is decomposed as

$$\begin{aligned}
\Omega_\mu(P,q) &= \mathbf{1}\phi^{(1)}_\mu(P,q) + \frac{i}{\sqrt{2}}\gamma_\nu\phi^{(2)}_{\nu\mu}(P,q) \\
&\quad +\frac{i}{\sqrt{2}}\gamma_5\gamma_\nu\phi^{(3)}_{\nu\mu}(P,q).
\end{aligned} \tag{18}$$

The association of the coefficients $\phi^{(i)}$ with the coefficients $\Lambda^{(i)}$ of (12) is directly observed from the relationship between the solutions to the inhomogeneous and homogeneous Bethe-Salpeter equations given in (5). The substitution of (18) into the homogeneous equation (6) allows a description in the form of the eigenvalue equation

$$\int d^4K \Delta^{-1}_{ab}(P,K;q)\Phi^\nu_b(K,q) = \alpha(q^2)\Phi^\nu_a(P,q) \tag{19}$$

to be obtained. The quantity $\Delta^{-1}_{ab}(P,K;q)$ is defined as

$$\begin{aligned}
\Delta^{-1}_{ab}(P,K;q) \equiv\ & \frac{9}{2}\int \frac{d^4r}{(2\pi)^4}\frac{e^{-i(P-K)r}}{g^2D(r)}\delta_{ab} \\
&+\delta^{(4)}(P-K)\mathrm{tr}\left[M^a G(K_+) M^b G(K_-)\right]
\end{aligned} \tag{20}$$

and plays the role of an inverse propagator for the $q\bar{q}$ composite system, as has been demonstrated in previous work on the hadronization of quark field-theory models [10]. That description is extended here to include the more general structure in (18). The eigenfunctions are defined in terms of the coefficient functions $\phi^{(i)}$ as

$\Phi_1^\nu \equiv \phi_\nu^{(1)}$, $\Phi_{2-5}^\nu \equiv \phi_{\alpha\nu}^{(2)}$, and $\Phi_{6-9}^\nu \equiv \phi_{\alpha\nu}^{(3)}$. The matrices $M^a \equiv \mathbf{1}_C \mathbf{1}_F \{\mathbf{1}, i\gamma_\mu/\sqrt{2}, i\gamma_5\gamma_\mu/\sqrt{2}\}$ include unity in the color and two-component flavor space, and the trace is taken to include their indices as well as those of the Dirac matrices. The homogeneous equation (6) is regained through the requirement that the eigenvalue vanishes on the mass shell, that is, $\alpha(q^2 = -M_V^2) = 0$. The normalization condition for the eigenfunctions is obtained by multiplying (18) on the left by $\Phi_a^\mu(P,-q)$ and integrating over relative momentum P, which gives

$$\int d^4P d^4K \Phi_a^\mu(P,-q)\Delta_{ab}^{-1}(P,K;q)\Phi_b^\nu(K,q) = \alpha(q^2)\int d^4P \Phi_a^\mu(P,-q)\Phi_a^\nu(P,q)$$
$$\overset{q^2\sim -M_V^2}{=} \left(\delta_{\mu\nu} - \frac{q_\mu q_\nu}{q^2}\right)(q^2 + M_V^2)\, Z(q^2). \tag{21}$$

The last line in (20) follows from the fact that the on-mass-shell eigenfunctions Φ_a^μ contain only components transverse to the center-of-mass momentum q_μ. The (dimensionless) wave-function renormalization constant $Z(q^2)$ can be absorbed into the Bethe-Salpeter amplitudes by defining $\hat{\Phi}_a^\nu \equiv \Phi_a^\nu/\sqrt{Z(-M_V^2)}$. The normalization condition can then be written explicitly as

$$\frac{1}{3}\int d^4P d^4K \hat{\Phi}_a^\nu(P,-q)\frac{\partial}{\partial q_\mu}\left[\Delta_{ab}^{-1}(P,K;q)\right]\hat{\Phi}_b^\nu(K,q)\Big|_{q^2=-M_V^2} = 2q_\mu, \tag{22}$$

which is the standard result [11]. In terms of the properly normalized Bethe-Salpeter amplitude, the relationship to the QPV given in (5) now reads

$$\Gamma_\mu(P,q) \approx \frac{M_V^2}{q^2 + M_V^2}\frac{\hat{\Omega}_\mu(P,q)}{f_V}, \tag{23}$$

where $f_V \equiv 1/\sqrt{Z(-M_V^2)}$ is the effective coupling of the vector meson to the photon.

III. A SIMPLE MODEL

Traditional descriptions of quark confinement are based on a potential between quarks, in an appropriate color combination, which rises with increasing separation (to infinity in the absence of pair creation). Explored here is the notion that this effect may be in part due to the interaction of quarks (or more generally colored objects) with the vacuum. In particular, that confinement is manifest in the absence of a mass pole in the vacuum Green's function of a colored object implies that the object is repelled by the vacuum, and hence attracted to other colored objects to form a color singlet by virtue of the interaction with the vacuum. An illustration of this mechanism is afforded through the use of a simple model [12, 8] of the gluon two-point function given by

$$D\left((P-K)^2\right) = \frac{3\eta^2\pi^4}{g^2}\delta^{(4)}(P-K). \tag{24}$$

At the present level of approximation, the self-energy dressing from the vacuum is provided by Eqs. (8) and (9). The solutions to these implied by (24) are

$$A(P^2) = \begin{cases} 2, & P^2 \le \frac{\eta^2}{4}, \\ \frac{1}{2}\left[1 + \left(1 + \frac{2\eta^2}{P^2}\right)^{\frac{1}{2}}\right], & P^2 \ge \frac{\eta^2}{4}, \end{cases}$$

$$B(P^2) = \begin{cases} (\eta^2 - 4P^2)^{\frac{1}{2}}, & P^2 \le \frac{\eta^2}{4}, \\ 0, & P^2 \ge \frac{\eta^2}{4}. \end{cases} \tag{25}$$

That the solutions (25) produce a model of confinement as described above can be seen by the absence of a solution to the expression $P^2 + M^2(P^2) = 0$, with $M = B/A$. The presence of other colored objects in a color singlet configuration can supply the additional interaction necessary for the formation of a propagating mode, as is demonstrated in the nontopological soliton model of Ref. [8]. There, for example, in the case of quarks coupled to a *constant* scalar mean field by the self-energy function B, the quark inverse Green's function obtains the form $G^{-1}(P) = i\not{P}A(P^2) + B(P^2)(1+\chi)$, where $0 \ge \chi \ge -2$ characterizes the strength of the mean field. In this case a *continuous* single-particle energy spectrum $E^2(\mathbf{P}^2) = \mathbf{P}^2 + M_C^2$ is obtained because of the infinite-range potential, with the constituent mass given by

$$M_C^2 = \frac{\eta^2}{4}\frac{(1+\chi)^2}{1-(1+\chi)^2}. \tag{26}$$

From (26) it is evident that the increase of the constituent mass as the strength χ of the mean field decreases toward its vacuum value ($\chi = 0$) is due to the repulsive interaction with the vacuum. For the case of the constant mean field, the quarks are allowed to propagate throughout space. However, due to the energy stored in the mean field, the self-consistent (minimum-energy) solution acquires a finite range. In that case, as a quark in the system is separated from the others, the influence of the mean field on the quark diminishes and the mass rises as in (26). The quarks are thus confined to the region of nonzero mean field by virtue of their interaction with the vacuum.

The situation is similar for the QPV of interest here. The use of the gluon two-point function (24) reduces the equations in (17) to algebraic form, which can then be solved by numerical or symbolic techniques. Shown in Fig. 3 is the solutions for the five transverse coefficient functions in both the timelike and spacelike regions of photon momentum q^2 for $P^2 = C_{Pq} = 0$. The single parameter, and the only dimensionful constant, η is given the value 5 fm^{-1}. It appears from Fig. 3(a) that there is

a pole for $q^2 = -\eta^2/2$. Closer analysis of the q^2-P^2 plane shows, however, that the singularity structure is not a discrete pole, but is instead a continuous spectrum. For the region $P_\pm^2 \leq \eta^2/4$, the analytic solutions have the simple form

$$\begin{aligned}
\lambda_1^T &= \frac{4\eta\left[B(P_+^2)+B(P_-^2)\right]}{\eta^2-4P^2+5q^2+B(P_+^2)B(P_-^2)}\,, \\
\lambda_2^T &= -\frac{q^2}{\eta^2}\lambda_4^T\,, \\
\lambda_3^T &= \frac{2\left[2\eta^2-4P^2+q^2+B(P_+^2)B(P_-^2)\right]}{3\eta^2-8P^2+6q^2}\,, \\
\lambda_4^T &= \frac{-32\eta^4}{\left[\eta^2-4P^2+5q^2+B(P_+^2)B(P_-^2)\right]\left[3\eta^2-8P^2+6q^2\right]}\,, \\
\lambda_5^T &= \frac{8\eta^2}{3\eta^2-8P^2+6q^2}\,,
\end{aligned} \tag{27}$$

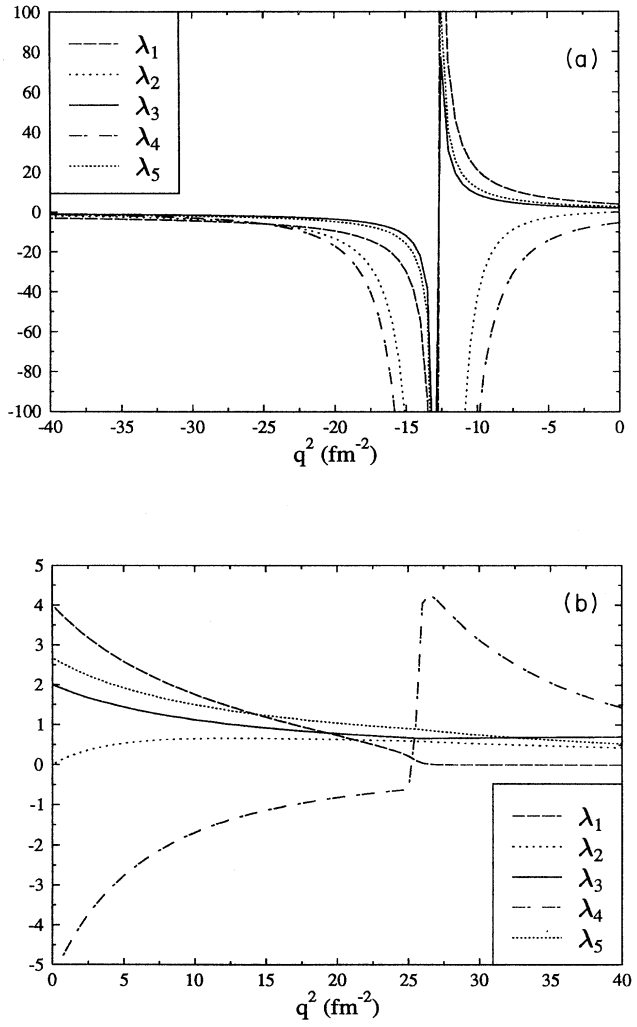

FIG. 3. The solutions for the five transverse coefficient functions λ_i^T obtained using the simple gluon two-point function described by Eq. (24) in the text, are plotted as a function of the photon momentum q^2 in both the (a) timelike and (b) spacelike regions for $P^2 = C_{Pq} = 0$.

from which the singularity structure is visible. The self-energy function B is given in (25). The analytic solutions outside this region are not as simple, but can be represented graphically. As an example, the coefficient function λ_3^T is shown in Fig. 4 for $C_{Pq} = 0$. The exhibited continuous spectrum arises from the fact that the gluon two-point function (24) provides a constant, or infinite-range, interaction between the quarks in coordinate space. The quarks are therefore allowed to propagate throughout space uninhibited by the presence of the vacuum. This situation is analogous to that of the constant mean-field case discussed previously.

Several observations can be made from this example. First, the absence of a mass pole in the vacuum Green's function of a colored object is sufficient for a description of confinement provided the subsequent interactions with other colored objects contain a scale beyond which the interaction diminishes allowing the presence of the vacuum to become apparent. This defines a confinement scale that is largely responsible for the characteristics of bound states. The effect of such a scale is investigated in the numerical work to follow in Sec. IV; however, one can

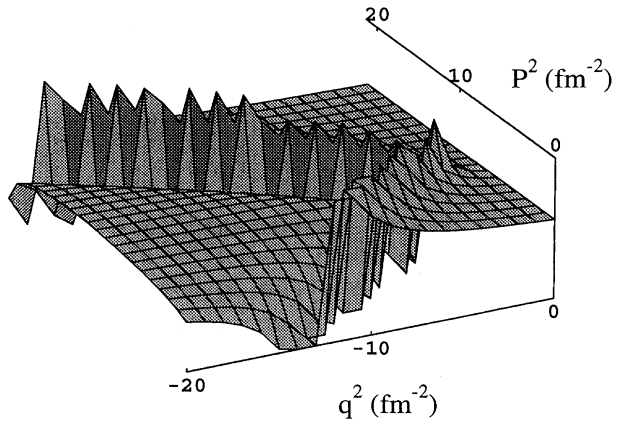

FIG. 4. The coefficient function λ_3^T is plotted in the $q^2 - P^2$ plane for $C_{Pq} = 0$. The variation of the singularity with P^2 is indicative of a continuous spectrum.

anticipate that as the range of the interaction increases, the density of bound-state poles increases, finally giving rise to a continuous spectrum as illustrated above. Second, the identification of a true bound-state pole requires careful examination of the P^2-q^2 plane. Finally, with regard to electron scattering, in general the singularity structure of the QPV in the timelike region of photon momentum squared dominates the behavior in the low momentum region of spacelike q^2. This feature is exhibited here despite the absence of a bound-state pole. The intercept at $q^2 = 0$ is provided by the constraints (16) derived from the WI, which the coefficient functions given in (27) satisfy explicitly. Further out in the spacelike region a transition to asymptotic behavior is expected. As is illustrated in Fig. 3(b), an unphysically sharp transition occurs here due to the nonanalytic structure of the self-energy amplitude B in (25). Based on these observations, the approximation (24) does not provide a useful description of bound states or the approach to asymptopia, but is of pedagogical value for investigating the behavior of the QPV for the situation where the confinement length scale, defined here as the quark separation at which the vacuum becomes apparent, is taken to infinity.

IV. NUMERICAL EVALUATION

A. Methods and approximations

The set of equations for the five transverse coefficient functions represented in (17), and given explicitly in the appendix, forms the basis for the numerical investigation undertaken here. The approach used in evaluating these equations is to express each *element* of the matrices (vectors) in the five-component space of coefficient functions as a *matrix* (*vector*) in the direct-product space of the magnitude of the momentum P and the direction cosine C_{Pq}. The value of the photon momentum q^2 is a parameter of the equations. That is, for each value of q^2, a different set of equations is obtained. For the numerical evaluation, the momentum P and the direction cosine C_{Pq} are discretized in terms of Gauss-quadrature points. The integrations are then carried out as matrix multiplication. The coupled equations are solved as a matrix equation in the expanded direct-product space of the coefficient functions and the Gauss integration points. The dimension of the equation is given by 5×npptsxncpts, where nppts and ncpts are the number of Gauss points representing the P and C_{Pq} integrations, respectively. The number of points in both integrations is varied to ensure accuracy. For the momentum, 20 to 40 quadrature points are used, while six to ten are used for the direction cosine.

1. Gluon two-point function ansatz

The aim in this initial investigation is not necessarily to reproduce the known bound-state spectrum, but rather to correlate trends in the spectrum with changes in the parameterization of the infrared form of the gluon two-point function. The sensitivity of the spectrum to these changes then provides a constraint on the calculation of the QPV in the spacelike region. To this end, a sufficient parametrization of the gluon two-point function is given by

$$g^2 D(P^2) = \frac{3\pi^2\eta^2}{16} R_0^4 e^{-R_0^2 P^2/4} + \frac{16\pi^2}{11 P^2 \ln(e + P^2/\Lambda^2)}, \tag{28}$$

where the first term (which has the coordinate space representation e^{-r^2/R_0^2}) provides a length scale R_0 characterizing the infrared behavior while the second term models the known ultraviolet form. The parameter Λ, which is associated with the QCD scale, is fixed at 1 fm^{-1} throughout this investigation. As R_0 approaches infinity the first term reduces to the delta-function model of Eq. (24). The gluon two-point function (28) has been employed previously in the study of Bethe-Salpeter and Schwinger-Dyson equations [4], and is expected to provide an acceptable accounting of the infrared effects for the purposes of the investigation conducted here.

2. Quark self-energy ansatz

The solution of the Bethe-Salpeter equation in the timelike region requires knowledge of the quark Green's functions, and hence the self-energy functions, for complex values of their arguments. The solution of the Schwinger-Dyson equation in the complex plane is a challenging problem in itself [13,7], and is being pursued elsewhere for forms such as that in (28) [14]. Although these solutions are crucial to a comprehensive study of the present problem, reasonable approximations are available. The analytic solutions given in (25) for the self-energy functions obtained using the simple model two-point function (24) are useful in this regard. It is shown, for example, in Ref. [4] that the solutions to (8) and (9) for the self-energy amplitudes obtained using (28) display behavior similar to the simple model solutions of (25) on the real axis with the exception of an additional tail on the scalar amplitude B attributed to the ultraviolet contribution in (28). Others have argued on both theoretical and experimental grounds that the asymptotic form of the scalar contribution to the self-energy should behave as $B(P^2) \sim 4m_D^3/P^2$, which, in the Landau gauge, is exact within a logarithm [15]. The self-energy functions used in the numerical work here are thus modeled as

$$A(P^2) = \begin{cases} 2, & P^2 \le \frac{\eta^2}{4}, \\ \frac{1}{2}\left[1 + \left(1 + \frac{2\eta^2}{P^2}\right)^{\frac{1}{2}}\right], & P^2 \ge \frac{\eta^2}{4}, \end{cases}$$

$$B(P^2) = \begin{cases} (\eta^2 - 4P^2)^{\frac{1}{2}} & P^2 \le \frac{\eta^2}{6}, \\ \frac{4m_D^3}{P^2}, & P^2 \ge \frac{\eta^2}{6}, \end{cases} \tag{29}$$

where the quantity m_D has been referred to previously as the "dynamical-quark mass"[15, 16], which sets the scale for dynamical chiral symmetry breaking. Its value is determined here by demanding that the function B and its first derivative match at the point $\eta^2/6$, and is thus given by $m_D = [24\sqrt{3}]^{-1/3}\eta \approx 0.29\eta$. For $\eta \sim 1$ GeV,

a dynamical-quark mass of $m_D \sim 290$ MeV is obtained, which is consistent with the notion of a constituent-quark mass. In Ref. [15], using evidence from e^+e^- annihilation, the dynamical mass is estimated to be $m_D \approx 244$ MeV. These arguments place constraints on the range of the parameter η, which is thereby fixed at 5 fm^{-1} (≈ 1 GeV) for the remainder of this work. The ansatz (29) encompasses the expected behavior of the solutions to the Schwinger-Dyson equation (2) on the real axis [7], and is here taken to define the solutions in the portion of the complex plane sampled by the QPV calculation.

B. Results

1. *Timelike q^2 and bound states*

Shown in Fig. 5 are the solutions to Eq. (17) for the five transverse coefficient functions in the timelike region

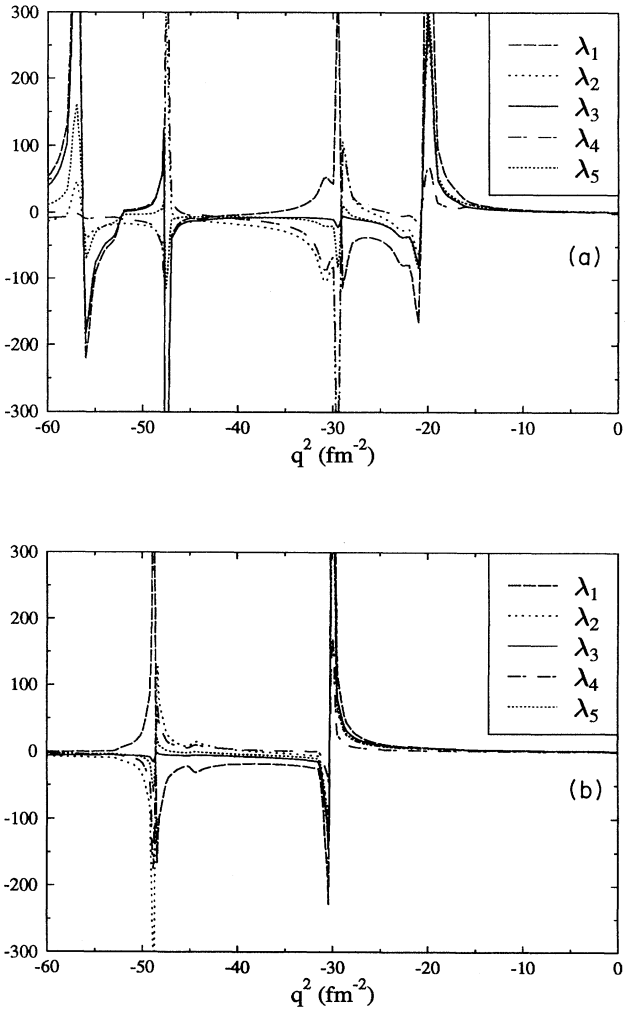

FIG. 5. The five transverse coefficient functions are plotted versus timelike photon momentum q^2 for $P^2 = C_{Pq} = 0$. The dependence upon the infrared scale R_0 is illustrated by comparing (a) where $R_0 = 1$ fm with (b) where $R_0 = 0.75$ fm.

of photon momentum squared. Two different values of the infrared scale R_0 are reported, from which it is observed that the spectrum is quite sensitive to changes in this parameter. In particular, an increase in R_0 leads to an increase in the density of bound-state poles. This situation is, for example, analogous to a potential well, where R_0 plays the role of the range while the barrier is provided by the repulsive interaction with the vacuum. With the value of R_0 set to 1 fm, the ground-state mass occurs at 880 MeV. This is in reasonable agreement with the observed ρ mass, considering that pion dressing is expected to lower this value [17], yet the excitation spectrum does not coincide with experimentally observed quantities. Comparison with the measured excitation spectrum can be improved by decreasing the range R_0; however, this also leads to an increase in the ground-state mass, and away from the known value. As illustrated previously with the analytic solutions (27), in the limit as R_0 approaches infinity a continuous spectrum is obtained. From this discussion, and the behavior displayed in Fig. 5, it is evident that the combination of the gluon two-point function (28) and the self-energy functions (29) is not sufficient to reproduce the empirical excitation spectrum. Nevertheless, it is encouraging that this approach affords the investigation of spectra beyond the ground state, which until recently [6] has been the focus of Bethe-Salpeter phenomenology applied to mesons. The reproduction of spectra is clearly essential to constraining the interaction between quarks. In this regard, the utility of the approach presented here is that, given a gluon two-point function and the associated solution to the Schwinger-Dyson equation, the vector bound-state spectrum can be obtained. The ability to reproduce the experimentally observed spectrum is then contingent upon the capacity of the ladder approximation to capture the relevant dynamics of QCD.

The extraction of bound-state wave functions is achieved by considering the dependence of the coefficient functions λ_i^T on the momentum P^2 and the direction cosine C_{Pq} in the vicinity of a pole. Shown in Fig. 6 are the solutions for the ground state with mass 880 MeV, and with $R_0 = 1$ fm, as a function of P^2 for the two limiting values of the direction cosine $C_{Pq} = 0, 1$. The normalization is chosen such that the largest coefficient function is unity at $P^2 = C_{Pq} = 0$. The relative strength of the other coefficients can then be observed. The absolute normalization is obtained through application of Eq. (22), but is not relevant to the present discussion. A rough estimate for the dependence of the solutions on the momentum and the direction cosine can be obtained by fitting the curves to an exponential of the form $e^{-P^2(1+aC_{Pq}^2)/\Delta^2}$, which gives $a \sim 0.29$ and $\Delta \sim 3.5$ fm^{-1}. The corresponding estimate of the spatial extent is $r_V \sim 2/\Delta \sim 0.57$ fm.

2. *Spacelike q^2 and electron scattering*

The description of the QPV in the spacelike region is largely independent of the spectrum in the timelike region with the exception of the ground state, which dominates the low momentum structure. The approach to

asymptotic behavior at higher momentum is primarily determined by the asymptotic forms of the gluon two-point function and the self-energy functions. Care has been taken here to accommodate both of these low and high momentum attributes in a manner that is consistent with their known features. The results of the calculation in the spacelike region are summarized in Figs. 7 and 8.

In Fig. 7 the solutions for the coefficient functions λ_i^T are displayed versus the photon momentum q^2 for $P^2 = C_{Pq} = 0$. A smooth transition from the low momentum region, dominated by the ground-state vector-meson pole, to the high momentum approach to asymptopia is observed. It is therefore expected that the range of applicability of these solutions spans the entire range of momentum transfers available in electron scattering experiments. With the exception of λ_3^T, which approaches unity asymptotically, the coefficient functions vanish for large momenta consistent with asymptotic freedom [9].

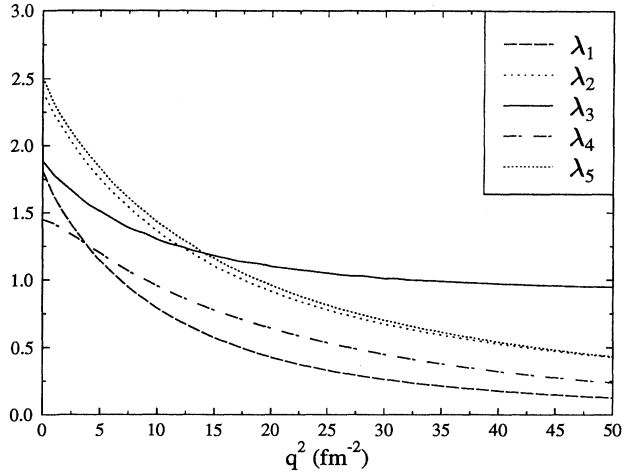

FIG. 7. The five transverse coefficient functions are plotted versus the photon momentum q^2 for $P^2 = C_{Pq} = 0$.

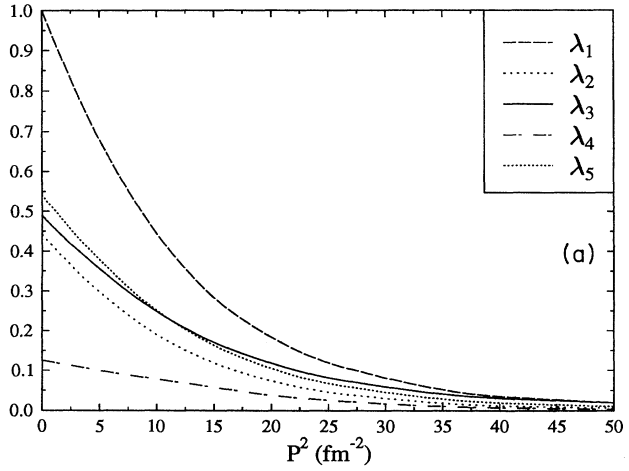

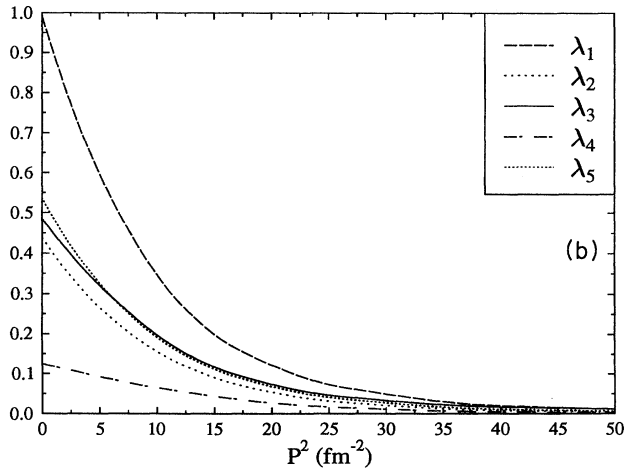

FIG. 6. The five transverse coefficient functions are plotted versus the momentum P^2 for values of the direction cosine (a) $C_{Pq} = 0$ and (b) $C_{Pq} = 1$, and for $-q^2 = M_V^2 = (880\ \text{MeV})^2$.

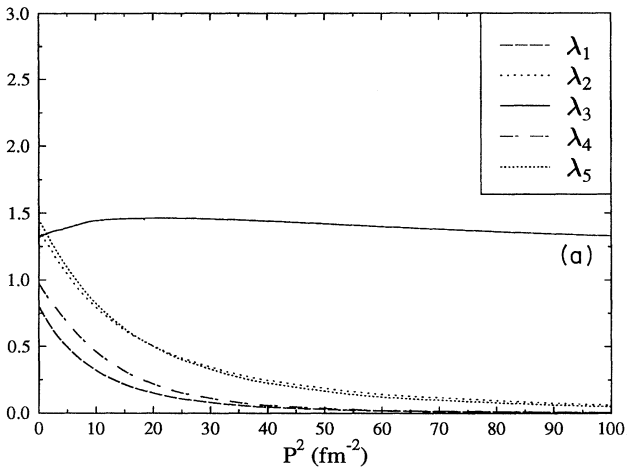

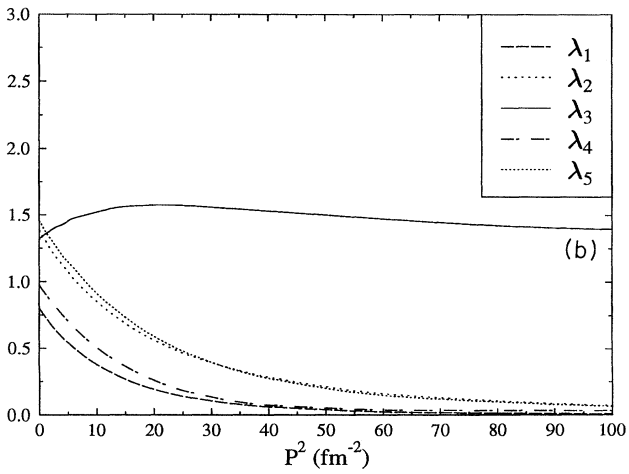

FIG. 8. The five transverse coefficient functions are plotted versus the momentum P^2 for photon momentum $q^2 = 10$ fm^{-2}, and the limiting values of the direction cosine (a) $C_{Pq} = 0$ and (b) $C_{Pq} = 1$.

The asymptotic form is apparent at $q^2 \sim 50$ fm^{-2} (~ 2 GeV^2), where the coefficient function λ_3^T achieves roughly twice the strength of the other coefficients. It is also worth pointing out that to a very good approximation the coefficients λ_2^T and λ_5^T are equal over the momentum range reported.

Shown in Fig. 8 are the coefficient functions versus the momentum P^2 for $q^2 = 10$ fm^{-2}, and for the limiting values of the direction cosine, $C_{Pq} = 0, 1$. Only a modest angular dependence is apparent, and again the coefficients λ_2^T and λ_5^T are approximately equal. The observed behavior in the spacelike region can be roughly characterized in terms of the scales of the problem by the following analytic forms:

$$\lambda_i^T \approx a_i \frac{1}{1+q^2/M_\rho^2} \frac{1}{1+P^2/(4m_D^2)} \left[\ln(e+(P^2+q^2/4)/\Lambda^2)\right]^{-1/2} \quad , \; i \neq 3 \; ,$$
$$\lambda_3^T \approx 1 + \frac{1}{1+q^2/M_\rho^2} \left[\ln(e+(P^2+q^2/4)/\Lambda^2)\right]^{-1/2} , \tag{30}$$

where the constants a_i can be read from Fig. 7, and in the present case the ground-state vector mass is $M_\rho = 880$ MeV. The falloff with the momentum P^2 is reminiscent of the self-energy functions, while that with q^2 reflects the presence of the singularity in the timelike region. It should be understood that these forms are not the result of a detailed fit, but are rather offered as a guide to the qualitative behavior over the momentum range reported.

V. SUMMARY

The inhomogeneous Bethe-Salpeter equation in the ladder approximation has been used to study several issues that arise in the nonperturbative description of the electromagnetic interaction with quarks. Specifically, the investigation presented here addresses aspects of this problem associated with confinement, asymptotic freedom, and the dynamical generation of $q\bar{q}$ vector meson modes in an electromagnetic gauge invariant formulation. The notion that confinement is manifest in the absence of a mass pole in the vacuum Green's function of a colored object is explored and is implemented for quarks through the Schwinger-Dyson equation in the rainbow approximation for their self-energy. The generation of $q\bar{q}$ vector meson modes is observed in the solutions of the inhomogeneous Bethe-Salpeter equation for timelike photon momentum squared, and their effect on the solutions for spacelike momentum is studied. The asymptotic behavior of the solutions for large spacelike momentum is also investigated and is shown to be consistent with asymptotic freedom. A detailed account of the numerical results is presented in the preceding section, while a summary of the qualitative features is given here.

The solution in the timelike region warrants further study, particularly with regard to the reproduction of the excitation spectrum. Nevertheless, the description presented here shows promise in the ability to study the vector meson spectrum beyond the ground state. Further, the sensitivity of the spectrum to the introduced infrared scale, which is demonstrated in Fig. 5, has positive implications for constraining the largely unknown behavior of the gluon two-point function at low momentum. In particular, the simple Gaussian ansatz ($e^{-R_0^2 P^2/4}$) employed here for this low-momentum behavior obtains an increase in the density of vector bound state poles as the interaction range R_0 increases, and finally gives a continuous spectrum in the limit as R_0 approaches infinity. In this limit analytic solutions are available and are given in Sec. III. The emergence of a continuous spectrum is somewhat surprising for particles which are supposed to be confined. This result in fact demonstrates that the absence of a mass pole in the vacuum Green's function of a colored object is alone not sufficient for a model of confinement but requires in addition that the subsequent interaction with other colored objects is finite ranged. Simply stated, the absence of a mass pole in the vacuum Green's function of a colored object implies that it is repelled by the vacuum. It is shown here, through the simple model illustration of Sec. III and the numerical solutions of Sec. IV, that the generation of confined $q\bar{q}$ states in such a description requires an interaction between the vacuum-dressed quarks which diminishes with their separation allowing the vacuum repulsion to become apparent. Here the gluon two-point function (28) with an interaction range $R_0 = 1.0$ fm obtains a $q\bar{q}$ vector ground-state mass $M_V = 880$ MeV with the residue at the pole displayed in Fig. 6. The estimated spatial extent is $r_V \sim 0.57$ fm. It should be emphasized that these results do not include meson dressing. The effect of varying the interaction range in this study illustrates how constraints on the low-momentum form of the gluon two-point function might be imposed through the investigation of spectra. The utility of this approach is, however, contingent upon the ability of the ladder approximation to capture the relevant bound-state dynamics of QCD.

The solution in the spacelike region is potentially the most useful result of this investigation. The quark-based study of the EM properties of hadrons relies heavily on the capacity to describe the quark-photon interaction. Modeling this quantity based on gauge invariance alone provides only partial constraints on its behavior, and in particular allows for arbitrariness in the components transverse to the four momentum of the photon, which are those probed by electron scattering experiments. The use of vector meson dominance or the bare QPV, is limited by the momentum range for which these approximations are sensible. Here a somewhat more fundamental approach has been taken by describing the quark-photon interaction through a model in which the dynamics dictates the role of $q\bar{q}$ vector bound states and the asymptotic behavior. The transverse contributions to the QPV

are thus uniquely defined within the employed ladder approximation to the inhomogeneous Bethe-Salpeter equation, and no restrictions on the momentum range are implied. The solutions in the spacelike region, shown in Figs. 7 and 8, are influenced by the singularity structure in the timelike region at low photon momentum, while at large photon momentum they are consistent with the expected asymptotic form. That is, the solutions approach the bare vertex at large photon momentum. The smooth transition between these low and high momentum regions provides useful information about the structure of photon-hadron vertices, for example, through the diagram of Fig. 1. The solutions obtained here are therefore expected to provide an essential ingredient in the quark-based description of the EM interactions with hadrons.

ACKNOWLEDGMENTS

The author wishes to thank C.D. Roberts, P.C. Tandy, M. Burkardt, and M. Herrmann for helpful conversations. This work was supported by the Department of Energy under Grant No. DE-FG06-90ER40561.

APPENDIX: DETAILS OF EQ. (17)

The essential steps required to reduce the inhomogeneous Bethe-Salpeter equation (1) to the matrix form given in (17) are listed below. To begin, the coefficient functions are isolated using (12) and (14), and the orthogonality of the Dirac matrices to obtain

$$\begin{aligned}
\frac{(P^T)^2}{\eta^2}\lambda_1^T &= \frac{1}{4}\frac{P_\mu^T}{\eta}\mathrm{tr}\left[\Gamma_\mu(P,q)\right] , \\
\frac{(P^T)^2}{\eta^2}\lambda_2^T - 3\lambda_3^T &= -\frac{i}{4}\left(\delta_{\mu\nu} - \frac{q_\mu q_\nu}{q^2}\right)\mathrm{tr}\left[\gamma_\nu\Gamma_\mu(P,q)\right] , \\
\frac{(P^T)^2}{\eta^2}\lambda_2^T - \lambda_3^T &= -\frac{i}{4}\frac{P_\mu^T P_\nu^T}{(P^T)^2}\mathrm{tr}\left[\gamma_\nu\Gamma_\mu(P,q)\right] , \\
\frac{P\cdot q}{\eta^2}\lambda_2^T + \frac{q^2 P\cdot q}{\eta^4}\lambda_4^T &= -\frac{i}{4}\frac{P_\mu^T q_\nu}{(P^T)^2}\mathrm{tr}\left[\gamma_\nu\Gamma_\mu(P,q)\right] , \\
\frac{q^2(P^T)^2}{\eta^4}\lambda_5^T &= -\frac{i}{8}\epsilon_{\mu\nu\alpha\beta}\frac{P_\alpha q_\beta}{\eta^2}\mathrm{tr}\left[\gamma_\nu\gamma_5\Gamma_\mu(P,q)\right] .
\end{aligned} \tag{A1}$$

The right-hand side of the equations in (A1) are evaluated using the inhomogeneous Bethe-Salpeter equation (1) for Γ_μ.

The remaining obstacle is the evaluation of the four-dimensional integration present in (1), which upon substitution into (A1) produces expressions of the form

$$\mathcal{I} \equiv \int d^4K\hat{D}\left(P^2+K^2-2PK\sqrt{1-C_{Pq}^2}C_{KT} - 2PKC_{Pq}C_{Kq}\right)C_{KT}^n F\left(P^2,K^2,q^2,C_{Kq},C_{Pq}\right) , \tag{A2}$$

where $n = 0,1,2$; $C_{Kq}(C_{KT})$ is the direction cosine between K and $q(K$ and $P^T)$; and $\hat{D}((P-K)^2) \equiv g^2D((P-K)^2)/\left(3\eta^2\pi^4\right)$. Here F is a generic function representing the integrands obtained from (A1). Since the vectors P_μ^T and q_μ are orthogonal, they can be used to define two of the four axes of integration. Rewriting the integration as

$$\int d^4K = 2\int_0^\infty dK K^3\int_{-1}^1 dC_{Kq}dC_{KT}dC_1dC_2\delta(1-C_{Kq}^2-C_{KT}^2-C_1^2-C_2^2), \tag{A3}$$

where C_1 and C_2 are the remaining direction cosines, we obtain from (A2) the result

$$\mathcal{I} = 2\pi\int_0^\infty dK K^3\int_{-1}^1 dC_{Kq}F\left(P^2,K^2,q^2,C_{Kq},C_{Pq}\right)\hat{D}_n(P^2,K^2,C_{Pq},C_{Kq}), \tag{A4}$$

where

$$\hat{D}_n(P^2,K^2,C_{Pq},C_{Kq}) \equiv \int_{-x}^{x} dC_{KT}\hat{D}\left(P^2+K^2-2PK\sqrt{1-C_{Pq}^2}C_{KT} - 2PKC_{Pq}C_{Kq}\right)C_{KT}^n, \tag{A5}$$

and $x \equiv \sqrt{1-C_{Kq}^2}$.

The explicit form of the quantities in (17) is listed below. The vector b is given by

$$b = (0,3,1,0,0). \tag{A6}$$

The matrix $\mathcal{N}$ is given by

$$\begin{aligned}
&\mathcal{N}_{11}=1 \quad \mathcal{N}_{22}=-\tfrac{(P^T)^2}{\eta^2}\ ,\\
&\mathcal{N}_{23}=3 \quad \mathcal{N}_{32}=-\tfrac{(P^T)^2}{\eta^2}\ ,\\
&\mathcal{N}_{33}=1 \quad \mathcal{N}_{42}=1\ ,\\
&\mathcal{N}_{44}=\tfrac{q^2}{\eta^2} \quad \mathcal{N}_{55}=1,
\end{aligned} \tag{A7}$$

where all other elements are zero. The matrix $\mathcal{M}$ is given by

$$\begin{aligned}
&\mathcal{M}_{11}=2\pi\hat{D}_1F_0\tfrac{K}{P^T}\ , && \mathcal{M}_{12}=2\pi\hat{D}_1\tfrac{K^3}{P^T\eta^2}\left(V+\tfrac{q^2}{\eta^2}C_{Kq}^2W\right)\ ,\\
&\mathcal{M}_{13}=-2\pi\hat{D}_1\tfrac{K}{P^T}V\ , && \mathcal{M}_{14}=2\pi\hat{D}_1\tfrac{K^3qr}{P^T\eta^4}C_{Kq}^2\left(V+\tfrac{q^2}{\eta^2}W\right)\ ,\\
&\mathcal{M}_{21}=-\pi\hat{D}_0\tfrac{K^2}{\eta^2}x^2V\ , && \mathcal{M}_{22}=\pi\hat{D}_0\tfrac{K^2}{\eta^2}x^2\left(F_1-2\tfrac{K^2}{\eta^2}T\right)\ ,\\
&\mathcal{M}_{23}=-\pi\hat{D}_0\left(3F_1-2\tfrac{K^2}{\eta^2}x^2T\right)\ , && \mathcal{M}_{24}=-2\pi\hat{D}_0\tfrac{K^4q^2}{\eta^6}x^2C_{Kq}^2T\ ,\\
&\mathcal{M}_{25}=2\pi\hat{D}_0\tfrac{K^2q^2}{\eta^4}x^2T\ , && \mathcal{M}_{31}=-\pi\hat{D}_2\tfrac{K^2}{\eta^2}V\ ,\\
&\mathcal{M}_{32}=\pi\hat{D}_2\tfrac{K^2}{\eta^2}\left(F_1-2\tfrac{K^2}{\eta^2}T\right)\ , && \mathcal{M}_{33}=-\pi\left(F_1\hat{D}_0-2\tfrac{K^2}{\eta^2}T\hat{D}_2\right)\ ,\\
&\mathcal{M}_{34}=-2\pi\hat{D}_2\tfrac{K^4q^2}{\eta^6}C_{Kq}^2T\ , && \mathcal{M}_{35}=\pi\left(\hat{D}_0x^2-\hat{D}_2\right)\tfrac{K^2q^2}{\eta^4}T\ ,\\
&\mathcal{M}_{41}=\pi\hat{D}_1\tfrac{K^2}{P^LP^T}C_{Kq}\left(V+\tfrac{q^2}{\eta^2}W\right), && \mathcal{M}_{42}=-\pi\hat{D}_1\tfrac{K^2}{P^LP^T}C_{Kq}F_2\ ,\\
&\mathcal{M}_{43}=-2\pi\hat{D}_1\tfrac{K^2}{P^LP^T}C_{Kq}T\ , && \mathcal{M}_{44}=-\pi\hat{D}_1\tfrac{K^2}{P^LP^T}C_{Kq}\tfrac{q^2}{\eta^2}F_3\ ,\\
&\mathcal{M}_{53}=-\pi\hat{D}_1\tfrac{K}{P^T}T\ , && \mathcal{M}_{55}=\pi\hat{D}_1\tfrac{K}{P^T}F_0\ ,
\end{aligned} \tag{A8}$$

where all unlisted elements are zero, and

$$\begin{aligned}
&F_0\equiv\left(\tfrac{q^2}{4}-K^2\right)\tfrac{1}{\eta^2}T+U\ , && F_1\equiv\left(K^2-\tfrac{q^2}{4}\right)\tfrac{1}{\eta^2}T+U\ ,\\
&F_2\equiv F_1+2\left(\tfrac{q^2}{4}-K^2\right)\tfrac{1}{\eta^2}T\ , && F_3\equiv F_1+2\left(\tfrac{q^2}{4}-K^2C_{Kq}^2\right)\tfrac{1}{\eta^2}T\ ,\\
&T\equiv\eta^4\alpha(K_+^2)\alpha(K_-^2)\ , && U\equiv\eta^2\beta(K_+^2)\beta(K_-^2)\ ,\\
&V\equiv\eta^3\left[\alpha(K_+)\beta(K_-)+\alpha(K_-)\beta(K_+)\right], && W\equiv\eta^5\left[\tfrac{\alpha(K_+)\beta(K_-)-\alpha(K_-)\beta(K_+)}{2K\cdot q}\right]\ .
\end{aligned} \tag{A9}$$

The quantities α and β are defined in (10); T, U, V, and W are dimensionless functions of K^2, q^2 and C_{Kq}^2; and the components of the momentum P are defined as $P_L \equiv PC_{Pq}$ and $P_T \equiv P\sqrt{1-C_{Pq}^2}$.

[1] N. Isgur, in *From Fundamental Fields to Nuclear Phenomena*, J.A. McNeil and C.E. Price (World Scientific, Singapore, 1991), pp. 46–54; R.L. Jaffe and P.F. Mende, Nucl. Phys. **B369**, 189 (1992).

[2] M.R. Frank and P.C. Tandy, Phys. Rev. C **49** (1994).

[3] R.T. Cahill, C.D. Roberts, and J. Praschifka, Phys. Rev. D **36**, 2804 (1987).

[4] J. Praschifka, R.T. Cahill, and C.D. Roberts, Int. J. Mod. Phys. A **4**, 4929 (1989).

[5] K.-I. Aoki, T. Kugo, and M.K. Mitchard, Phys. Lett. B **266**, 467 (1991).

[6] H.J. Munczek and P. Jain, Phys. Rev. D **46**, 438 (1992); P. Jain and H.J. Munczek, *ibid.* **48**, 5403 (1993).

[7] C.D. Roberts and A.G. Williams, Prog. Part. Nucl. Phys. **33**, 477 (1994).

[8] M.R. Frank, P.C. Tandy, and G. Fai, Phys. Rev. C **43**, 2808 (1991); P.C. Tandy and M.R. Frank, Aust. J. Phys. **44**, 181 (1991); M.R. Frank and P.C. Tandy, Phys. Rev. C **46**, 338 (1992).

[9] W. Marciano and H. Pagles, Phys. Rep. C **36**, 137 (1978).

[10] R.T. Cahill, Aust. J. Phys. **42**, 171 (1989).

[11] C. Itzykson and J.-B. Zuber, *Quantum Field Theory* (McGraw-Hill, New York, 1980).

[12] H.J. Munczek and A.M. Nemirovsky, Phys. Rev. D **28** (1983); R.T. Cahill and C.D. Roberts, *ibid.* **32**, 2419 (1985); C.M. Shakin, Ann. Phys. **192**, 254 (1989).

[13] C.J. Burden, C.D. Roberts, and A.G. Williams, Phys. Lett. B **285**, 347 (1992).

[14] Conrad Burden (private communication).

[15] H. Pagels and S. Stokar, Phys. Rev. D **20**, 2947 (1979).

[16] R.T. Cahill and C.D. Roberts, Phys. Rev. D **32**, 2419 (1985).

[17] L.C.L. Hollenberg, C.D. Roberts, and B.H.J. McKellar, Phys. Rev. C **46**, 2057 (1992); M. Herrmann, B.L. Friman, and W. Nörenberg, Nucl. Phys. **A560**, 411 (1993).